PLOS COMPUTATIONAL BIOLOGY

RESEARCH ARTICLE

Primacy coding facilitates effective odor discrimination when receptor sensitivities are tuned

David Zwicker[1,2,3]*

1 Max Planck Institute for Dynamics and Self-Organization, Göttingen, Germany, **2** John A. Paulson School of Engineering and Applied Sciences, Harvard University, Cambridge, Massachusetts, United States of America, **3** Kavli Institute for Bionano Science and Technology, Harvard University, Cambridge, Massachusetts, United States of America

* david.zwicker@ds.mpg.de

Check for updates

OPEN ACCESS

Citation: Zwicker D (2019) Primacy coding facilitates effective odor discrimination when receptor sensitivities are tuned. PLoS Comput Biol 15(7): e1007188. https://doi.org/10.1371/journal.pcbi.1007188

Editor: Peter E. Latham, UCL, UNITED KINGDOM

Received: December 5, 2018

Accepted: June 17, 2019

Published: July 19, 2019

Copyright: © 2019 David Zwicker. This is an open access article distributed under the terms of the Creative Commons Attribution License, which permits unrestricted use, distribution, and reproduction in any medium, provided the original author and source are credited.

Data Availability Statement: The python source code for the simulations in this paper is available at https://github.com/david-zwicker/sensing.

Funding: This work was funded by the Simons Foundation and the German Science Foundation through ZW 222/1-1. The funders had no role in study design, data collection and analysis, decision to publish, or preparation of the manuscript.

Competing interests: The author has declared that no competing interests exist.

Abstract

The olfactory system faces the difficult task of identifying an enormous variety of odors independent of their intensity. Primacy coding, where the odor identity is encoded by the receptor types that respond earliest, might provide a compact and informative representation that can be interpreted efficiently by the brain. In this paper, we analyze the information transmitted by a simple model of primacy coding using numerical simulations and statistical descriptions. We show that the encoded information depends strongly on the number of receptor types included in the primacy representation, but only weakly on the size of the receptor repertoire. The representation is independent of the odor intensity and the transmitted information is useful to perform typical olfactory tasks with close to experimentally measured performance. Interestingly, we find situations in which a smaller receptor repertoire is advantageous for discriminating odors. The model also suggests that overly sensitive receptor types could dominate the entire response and make the whole array useless, which allows us to predict how receptor arrays need to adapt to stay useful during environmental changes. Taken together, we show that primacy coding is more useful than simple binary and normalized coding, essentially because the sparsity of the odor representations is independent of the odor statistics, in contrast to the alternatives. Primacy coding thus provides an efficient odor representation that is independent of the odor intensity and might thus help to identify odors in the olfactory cortex.

Author summary

Humans can identify odors independent of their intensity. Experimental data suggest that this is accomplished by representing the odor identity by the earliest responding receptor types. Using theoretical modeling, we here show that such a primacy code outperforms alternative encodings and allows discriminating odors with close to experimentally measured performance. This performance depends strongly on the number of receptors considered in the primacy code, but the receptor repertoire size is less important. The model

also suggests a strong evolutionary pressure on the receptor sensitivities, which could explain observed receptor copy number adaptations. By predicting psycho-physical experiments, the model will thus contribute to our understanding of the olfactory system.

Introduction

The olfactory system identifies and discriminates odors for solving vital tasks like navigating the environment, identifying food, and engaging in social interactions. These tasks are complicated by the enormous variety of odors, which vary in composition and in the concentrations of their individual molecules. In particular, the olfactory system needs to separately recognize the odor identity (what is there?) and the odor intensity (how much is there?). For instance, the identity is required to decide whether to approach or avoid an odor source, whereas the intensity information is important for localizing it. It is not understood how these two odor properties are separated and how odors are discriminated reliably.

Odors are comprised of chemicals that bind to and excite olfactory receptors in the nose in mammals and on antenna in insects. Each receptor responds to a wide range of odors and each odor activates many receptor types. The resulting combinatorial code allows to distinguish odor identities [1–3], but also depends on the odor intensity, since receptors respond stronger to more concentrated molecules [4]. To separate these two properties, the neural signals are processed in the olfactory bulb (antennal lobe in insects) and then forwarded to the olfactory cortex, where odors are identified by comparing to memorized patterns. Indeed, experiments indicate that the olfactory cortex receives a concentration-invariant code [5, 6], which allows to identify odors irrespective of their intensity. Consequently, the olfactory bulb can be thought of as a signal processor that removes statistical redundancies in the input to provide a more useful representation to the olfactory cortex. However, so far it is not clear what processing the olfactory bulb performs and how this affects odor representations.

The olfactory bulb contains neural clusters called glomeruli, which each receive input from a specific receptor type [7–9]. Each glomerulus excites associated projection neurons, which project into the olfactory cortex. Additionally, the glomeruli are connected by local neurons [10, 11], which inhibit the projection neurons [12–18]. These local neurons could mediate a global normalization resulting in an intensity-invariant representation of the odor identity [19, 20]. However, we showed that simple normalized representations still depend strongly on the number of ligands in a mixture and might thus not be optimal for solving olfactory tasks [21]. An alternative to these normalized representations is rank coding, where the order in which the receptors are excited is used to encode the odor identity robustly and independently of the odor intensity [22]. Indeed, experiments suggests that odors are encoded robustly by the receptor types that respond within a given time window after sniff onset [23–25]. In particular, the odor identity could be robustly encoded by a fixed number of the receptors that respond first, which is known as primacy coding [24, 26]. So far, it is unclear how efficient and useful primacy coding is and how it compares to alternative schemes.

In this paper, we consider a simple model of primacy coding and investigate how well it represents complex odors. In particular, we identify how much information is transmitted to the cortex and how well this information can be used to perform typical olfactory tasks, like identifying the addition of a target odor to a background or discriminating odor mixtures. Our statistical approach allows linking parameters of the primacy code to results from typical psychophysical experiments. We show that primacy coding provides a robust and compact representation of the odor identity over a wide range of odors, independent of the odor

intensity, and that it outperforms other simple coding schemes. However, this good performance of the olfactory system hinges on tuned receptor sensitivities, which suggests that there is a strong selective pressure to adjust the sensitivities on evolutionary and shorter timescales.

Results

We describe odors by concentration vectors $\boldsymbol{c} = (c_1, c_2, \ldots, c_{N_L})$, which determine the concentrations $c_i \geq 0$ of all ligands that can be detected by the olfactory receptors. The number N_L of possible ligands is at least $N_L = 2300$ [27] although the actual number is likely much larger [28]. Typical odors contain only tens to hundreds of ligands, implying that most c_i are zero.

In experiments, the olfactory system is typically characterized by presenting odors with particular statistics, e.g., by choosing mixtures from a given ligand library. Although such experiments allow to characterize the olfactory system in a part of odor space, we ultimately want to understand how the system performs in its natural environment. Unfortunately, the statistics of natural odors are difficult to measure [29], so we here consider a broad class of odor distributions to approximate natural odor statistics [30]. In particular, we consider a situation in which each ligand i has a probability p_i to appear in an odor. For simplicity, we neglect correlations in their appearance, so the mean number s of ligands in an odor is $s = \sum_i p_i$. To model the broad distribution of ligand concentrations, we choose the concentration c_i of ligand i from a log-normal distribution with mean μ_i and standard deviation σ_i if the ligand is present. Consequently, the mean concentration of a ligand in any odor reads $\langle c_i \rangle = p_i \mu_i$ and the associated variance is $\mathrm{var}(c_i) = (p_i - p_i^2)\mu_i^2 + p_i\sigma_i^2$. For simplicity, we consider ligands with equal statistics in this paper, so the distribution $P_{\mathrm{env}}(\boldsymbol{c})$ of odors is characterized by the three parameters $p_i = p$, $\mu_i = \mu$, and $\sigma_i = \sigma$. Using these broad odor statistics and more specific ones will allow us to analyze the performance of olfactory models in natural environments and in typical psychophysical experiments, respectively.

Simple model of primacy coding

Odors are detected by an array of receptors in the nasal cavity in mammals and on the antenna in insects. The receptor array consists of N_R different receptor types, which each are expressed many times. Typical numbers are $N_R \approx 50$ in flies [7], $N_R \approx 300$ in humans [31], and $N_R \approx 1000$ in mice [32]. The excitations of all receptors of the same type are accumulated in an associated glomerulus in the olfactory bulb in mammals and the antennal lobe in insects [33]. Since this convergence of the neural information mainly improves the signal-to-noise ratio, we here capture the excitation of the receptors at the level of glomeruli; see Fig 1A. The excitation e_n of glomerulus n can be approximated by a linear function of the odor $\boldsymbol{c}$ [4, 34],

$$e_n = \sum_{i=1}^{N_L} S_{ni} c_i \,, \tag{1}$$

where S_{ni} denotes the effective sensitivity of glomerulus n to ligand i. Note that S_{ni} is proportional to the copy number of receptor type n if the response from all individual receptors is summed [30].

The sensitivity matrix S_{ni} could in principle be determined by measuring the response of each glomerulus to each possible ligand. However, because the numbers of receptor and ligand types are large, this is challenging and only parts of the sensitivity matrix have been measured, e.g., in humans [35] and flies [36]. Using these data, we showed that the measured matrix elements are well described by a log-normal distribution with a standard deviation $\lambda \approx 1$ of the underlying normal distribution [30]. Motivated by these observations, we here consider

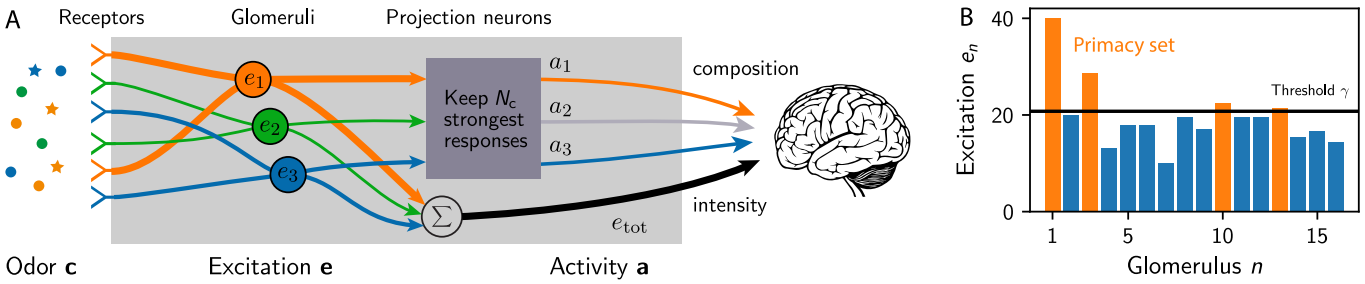

Fig 1. Simple model of primacy coding. (A) Schematic picture of the signal processing in the olfactory bulb: An odor comprised of many ligands excites the olfactory receptors and the signals from all receptors of the same type are accumulated in respective glomeruli. Under primacy coding, the glomeruli with the strongest (earliest) excitations encode the odor composition, whereas the odor intensity could be encoded separately. (B) Excitations of $N_R = 16$ glomeruli for an arbitrary odor. The $N_C = 4$ glomeruli with the highest excitations, above the threshold γ, form the primacy set (orange bars).

https://doi.org/10.1371/journal.pcbi.1007188.g001

random sensitivity matrices, where each element S_{ni} is chosen independently from the same log-normal distribution, which is parameterized by its mean $\langle S_{ni}\rangle = \bar{S}$ and variance $\mathrm{var}\,(S_{ni}) = \bar{S}^2(e^{\lambda^2} - 1)$ with $\lambda = 1$ [30]. Since these receptor sensitivities are broadly distributed, they might not include specific receptors related to innate behavior [37], but they can collectively discriminate concentration differences of several orders of magnitude [30].

The odor representation on the level of glomeruli excitations e_n depends strongly on the odor intensity, which is quantified by the total concentration $c_{\mathrm{tot}} = \Sigma_i\, c_i$. This dependency complicates the extraction of the odor identity, which is determined by the ligands which are present and their relative concentrations. A concentration-invariant representation could be achieved by normalizing the excitations by their mean [16], which leads to an efficient neural representation on the level of projection neurons [21]. However, recent experimental data suggest an alternative encoding based on the timing of the glomeruli excitation [24]. The key idea of this primacy coding is that the set of receptor types that are excited first is independent of the total concentration c_{tot} and thus provides a concentration-invariant representation.

In our simple model of primacy coding, odors are encoded by the identity of the N_C glomeruli that respond first. For simplicity, we here neglect the order in which they respond, in contrast to rank coding [22], and we also consider the simple situation where ligands binding to receptors only affect the magnitude of the receptor output, but not the signaling dynamics. In this case, receptors that respond first are also the ones with the largest excitation, so that the primacy code is given by the identity of the N_C glomeruli with the largest excitation, which is known as the primacy set [38].

The primacy set can be represented by a binary activity vector $\boldsymbol{a} = (a_1, a_2, \ldots, a_{N_R})$, where $a_n = 1$ implies that glomerulus n belongs to the primacy set and is active, while $a_n = 0$ denotes an inactive glomerulus not belonging to the primacy set. Since the active glomeruli have the highest excitation, they can be identified using an excitation threshold γ; see Fig 1B. Consequently, the activities are given by

$$a_n = \begin{cases} 1 & e_n > \gamma(\boldsymbol{e}) \\ 0 & e_n \leq \gamma(\boldsymbol{e}) \end{cases}. \tag{2}$$

Physiologically, the activities a_n could be encoded by projection neurons in insects and mitral and tufted cells in mammals. These neurons receive excitatory input from one glomerulus [39] and are inhibited by a local network of granule cells [20, 33]. These granule cells basically integrate the activity of all glomeruli [40] and could inhibit the glomeruli once a threshold is reached. Taken together, this would implement primacy coding since only the

glomeruli that respond earliest would be activated. For simplicity, we consider the case where the number N_C of active glomeruli is fixed and does not depend on the odor $\boldsymbol{c}$. The associated constraint

$$N_{\mathrm{C}} = \sum_{n=1}^{N_{\mathrm{R}}} a_n \tag{3}$$

determines the threshold γ. Note that the activity pattern $\boldsymbol{a}$ is sparse since only a fraction $N_{\mathrm{C}}/N_{\mathrm{R}}$ of all glomeruli is activated. Moreover, $\boldsymbol{a}$ is independent of $\bar{S}$ and c_{tot}, implying concentration-invariance. This is because multiplying the concentration vector $\boldsymbol{c}$ by a factor changes the excitations e_n and the threshold γ by the same factor, so that $\boldsymbol{a}$ given by Eq (2) is unaffected. In essence, only relative excitations are relevant for our model of primacy coding.

In the binary representation given by Eq (2), each receptor type can at most contribute 1 *bit* of information to the odor representation. This worst-case scenario corresponds to large processing noise, such that intermediate excitations cannot be identified in the downstream processing. In fact, the concentration range over which receptors are sensitive is typically small compared to the expected range of odorant concentrations [41]. Consequently, receptors will be activated either very little or very strongly for natural odors, suggesting a binary picture. Moreover, there is evidence that the identity of active neurons can robustly encode odor identity and is actually used in the olfactory system [5].

To see whether primacy coding encodes odor information efficiently [42], we quantify the amount of information I that can be learned about the odor $\boldsymbol{c}$ by observing the binary activity pattern $\boldsymbol{a}$ with given sparsity $N_{\mathrm{C}}/N_{\mathrm{R}}$. Since our model is deterministic, I is given by the entropy

$$I = -\sum_{\boldsymbol{a}} P(\boldsymbol{a}) \log_2 P(\boldsymbol{a}) \ , \tag{4}$$

where the probability $P(\boldsymbol{a})$ of observing an output $\boldsymbol{a}$ depends on the odor environment $P_{\mathrm{env}}(\boldsymbol{c})$ as well as the properties of the olfactory system, which in our model are quantified by N_{C}, N_{R}, and λ. Since further processing in the downstream regions of the brain can only reduce the amount of information, Eq (4) provides an upper bound for the information that the brain receives about odors when primacy coding as described by Eqs (1)–(3) is used.

In an optimal receptor array, each output $\boldsymbol{a}$ occurs with equal probability when encountering odors distributed according to $P_{\mathrm{env}}(\boldsymbol{c})$ [30]. In our model, only outputs with exactly N_{C} active receptor types are permissible. The resulting representations would be optimal if each receptor type was activated with a probability $\langle a_n \rangle = N_{\mathrm{C}}/N_{\mathrm{R}}$ and all types were uncorrelated, $\mathrm{cov}(a_n, a_m) = 0$ for $n \neq m$. The associated information

$$I_{\max}(N_{\mathrm{C}}, N_{\mathrm{R}}) = \log_2 \binom{N_{\mathrm{R}}}{N_{\mathrm{C}}} \approx \frac{N_{\mathrm{C}} - 1}{\ln 2} + N_{\mathrm{C}} \log_2 \frac{N_{\mathrm{R}}}{N_{\mathrm{C}}} \tag{5}$$

provides an upper bound for I given by Eq (4). Here, the approximation on the right hand side is obtained using Stirling's formula for large receptor repertoires ($N_{\mathrm{R}} \gg N_{\mathrm{C}}$).

Transmitted information depends weakly on receptor repertoire

We start by analyzing the information I transmitted by the primacy code using numerical ensemble averages of Eqs (1)–(4); see Methods and Models. Fig 2A shows that I is very close to the maximal information $I_{\max}$ given by Eq (5), which is obtained when all receptor types have equal activity and are uncorrelated [30]. This indicates that the primacy code uses the different receptor types with similar frequency and that correlations between them are negligible. The expression for $I_{\max}$ implies that the information grows linearly with the primacy dimension

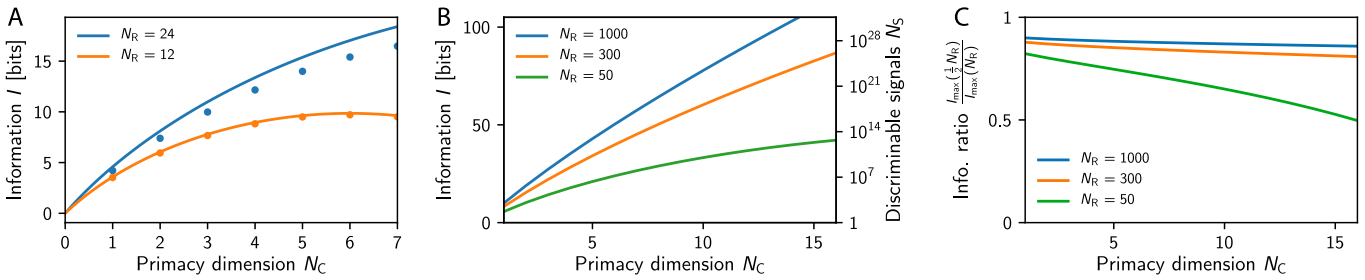

Fig 2. Transmitted information I increases strongly with primacy dimension N_C and weakly with receptor repertoire size N_R. (A) The maximally transmitted information I_{max} (solid lines) given by Eq (5) is compared to numerical estimates of I (dots; $n = 10^7$, error smaller than symbol size) obtained from ensemble averages of Eq (4). Model parameters are $N_L = 512$, $\mu = \sigma = 1$, $s = 16$, and $\lambda = 1$, implying $\zeta \approx 0.1$. (B) I_{max} as a function of N_C for several N_R. The right axis indicates the maximal number of distinguishable signals, $N_S = 2^I$. (C) Reduction of I_{max} when half the receptor types are removed as a function of N_C for various N_R.

https://doi.org/10.1371/journal.pcbi.1007188.g002

N_C, but only logarithmically with the number N_R of receptor types. Consequently, the number of distinguishable signals, $N_S = 2^I$, grows strongly with N_C, but the dependence on the repertoire size is weaker; see Fig 2B. Given equal N_C, our model thus predicts that the transmitted information in mice is only twice that of flies, although mice possess about 20 times as many receptor types. However, the number of discriminable signals changes by many orders of magnitudes, since it scales exponentially with I.

The logarithmic scaling of the transmitted information I with the receptor repertoire size N_R could explain why the ability of rats to discriminate odors is not significantly affected when half the olfactory bulb is removed in lesion experiments [43, 44]. If this operation removes half the receptor types, our model implies that the transmitted information I is lowered by N_C bits; see Eq (5). This corresponds to a reduction of I by about 10% in rats where $N_R \approx 1000$; see Fig 2C. Conversely, the transmitted information decreases by almost 50% in flies, which have a much smaller receptor repertoire of $N_R \approx 50$. Our model thus predicts that lesion experiments have a much more severe effect on the performance of animals with smaller receptor repertoires.

Taken together, this first analysis already suggests that the primacy code provides a robust odor representation, which is sparse, concentration-invariant, and depends only weakly on the details of the receptor array. However, for this representation to be useful to the animal, it needs to allow solving typical olfactory tasks.

Primacy coding discriminates odors efficiently

Typical olfactory tasks include detecting a ligand in a distracting background, detecting the addition of a ligand to a mixture, as well as discriminating similar mixtures. All these tasks involve discriminating odors with common ligands, implying that the associated primacy sets are correlated. This correlation can be quantified by the expected Hamming distance d between the primacy sets, which counts the number of glomeruli with different activities. The probability η that this distance is larger than 0, so that the two odor representations can be discriminated in principle, is given by

$$\eta(d) \approx 1 - \left(1 - \frac{d}{2N_C}\right)^{N_C}; \tag{6}$$

see Methods and Models. In particular, discriminating similar odors will be impossible ($\eta = 0$) if their primacy sets are identical ($d = 0$).

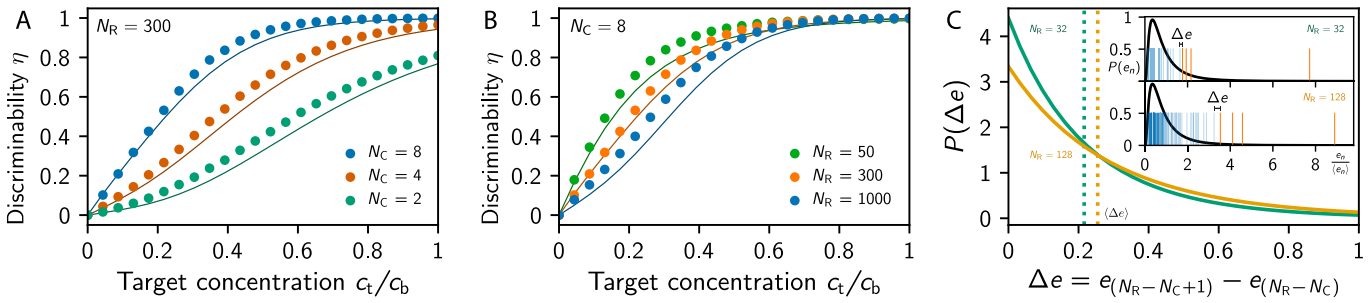

Fig 3. Detecting a target ligand in a background. (A-B) Probability η that adding a target odor at concentration c_t to a background ligand at concentration c_b can be detected using primacy coding as a function of c_t/c_b for (A) various N_C at $N_R = 300$ and (B) various N_R at $N_C = 8$. Numerical simulations (dots; sample size: 10^5) are compared to the theoretical prediction (lines) obtained using the statistical model; see Methods and Models. (C) Distribution of the difference Δe between the excitations just above and below the threshold for $N_R = 32$ (green line) and $N_R = 128$ (orange line); see Methods and Models. The dotted vertical lines indicate the mean $\langle \Delta e \rangle$, obtained from Eq (13). The inset shows $N_R = 32$ (upper panel) and $N_R = 128$ (lower panel) excitation realizations (vertical bars) drawn from the same excitation distribution (black lines). The orange bars indicate the primacy set consisting of the $N_C = 4$ largest excitations. (A–C) Remaining parameters are given in Fig 2A.

https://doi.org/10.1371/journal.pcbi.1007188.g003

Discriminating uncorrelated odors. To build an intuition for this analysis, we start by considering two uncorrelated odors. In this case, each receptor type has an expected activity of $\langle a_n \rangle = N_C/N_R$, implying the distance $d_* = 2N_C(1 - N_C N_R^{-1})$ and $\eta_* \approx 1 - (N_C/N_R)^{N_C}$. Our model thus predicts that uncorrelated odors can be discriminated almost surely ($\eta > 99.99\%$ for $N_C = 4$ and $N_R = 50$). The discriminability increases strongly with N_C, while the receptor repertoire size N_R has a much weaker effect in the typical case $N_C \ll N_R$, similar to the scaling of the information I discussed above. The value η_* marks the upper bound for the discriminability η, which can be much lower for correlated odors.

Detecting the presence of a target odor in a background. One simple task where odors are correlated is the detection of a target odor in a distracting background. To understand when a target can be detected, we analyze how the primacy set $\boldsymbol{a}$ changes when a single ligand at concentration c_t is added to a background ligand at concentration c_b. Because of concentration-invariance, the result only depends on the relative target concentration c_t/c_b. Fig 3A shows that the target is easier to detect when it is more concentrated (larger c_t/c_b) and when more receptor types participate in the primacy code (larger N_C). Conversely, the repertoire size N_R has only a weak influence, similar to the cases discussed above; see Fig 3B. Surprisingly, however, this figure also shows that dilute odors (small c_t/c_b) are more difficult to discriminate with larger receptor repertoires.

The fact that increasing the receptor repertoire size N_R can impede the detection of the target odor can be understood in a simplified statistical model, where we consider ensemble averages over sensitivity matrices; see Methods and Models. Since the primacy set $\boldsymbol{a}$ corresponds to the N_C receptor types with the largest excitations, $\boldsymbol{a}$ will only change when adding the target odor shuffles the excitations in the vicinity of the threshold γ. Intuitively, this is more likely when the associated excitation difference Δe is small. Fig 3C shows that Δe typically increases with N_R, essentially because the distribution of the glomeruli excitation e_n has a heavy tail, so that sampling more excitations leads to larger gaps between the largest excitations. These larger gaps in the excitations reduce the likelihood that adding the target changes the order of the excitations and thus the primacy set. Consequently, it is more difficult to detect the target using larger repertoires. Taken together, these arguments suggest that increasing the receptor repertoire is only beneficial if the primacy dimension Nc is also increased.

Detecting the addition of a ligand to a mixture. So far, we considered simple odors consisting of single ligands. However, realistic odors are comprised of many different ligands

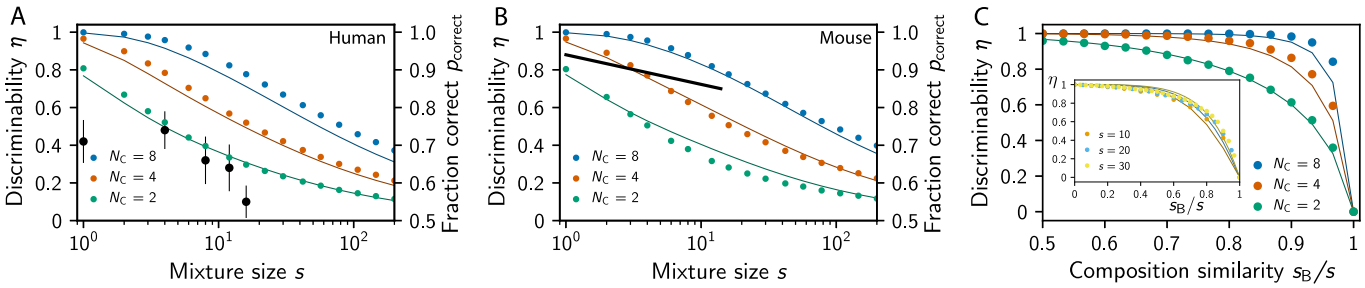

Fig 4. Discrimination of odor mixtures. (A,B) Probability η that adding a ligand to a mixture of s ligands changes the primacy set for various N_C. The right axes display the expected fraction $p_{correct}$ of correct responses in the respective go/no-go experiment. Theoretical predictions (colored symbols and lines) are compared to experimental data (black symbols and lines) for (A) humans ($N_R = 300$, data from [45]) and (B) mice ($N_R = 1000$, data from [46]). (C) Probability η that changing s_B ligands of a mixture of s ligands can be detected using primacy coding as a function of the composition similarity s_B/s for various N_C at $N_R = 300$, $s = 30$, and $\sigma^2/\mu^2 = 0$. The inset shows η as a function of s_B/s for various s at $N_C = 8$, $N_R = 300$, and $\sigma^2/\mu^2 = 10$. (A–C) Remaining parameters are given in Fig 2A.

https://doi.org/10.1371/journal.pcbi.1007188.g004

and target odors thus also need to be detected in backgrounds of many distracting ligands. Not surprisingly, experiments in humans [45] and mice [46] have shown that targets are more difficult to identify if the background consist of many ligands. In these experiments, subjects had to indicate whether a known odor is present or not in a presented odor mixture. The probability $p_{correct}$ of giving the correct answer is related to the probability η of obtaining enough olfactory information by $p_{correct} = \eta + \frac{1}{2}(1 - \eta)$ since there is a 50% chance of choosing the correct answer even if no information is present. In the following, we compare the experimentally measured values of $p_{correct}$ to the ones predicted by our model to restrict its parameters.

For simplicity, we first ask whether the primacy set changes when a ligand is added to a background, which is necessary for discriminating the background with the target from the background without it. This analysis will provide a theoretical upper bound for the performance, allowing us to restrict model parameters. In particular, we use ensemble averages over sensitivity matrices to compute η and $p_{correct}$ for the addition of a single ligand to a background consisting of s ligands, all at the same concentration. Fig 4A and 4B show that these values decrease both with larger mixture sizes s and smaller primacy dimension N_C. Conversely, whether the receptor repertoire size of humans ($N_R = 300$; Fig 4A) or that of mice ($N_R = 1000$, Fig 4B) is considered is irrelevant for the theoretical result, while the experimental data (black symbols and lines) are significantly different. Our model suggest that the superior performance of mice could be related to a larger primacy dimension N_C, although we cannot exclude the possibility that the decoding in higher regions of the brain is much more efficient in mice than in humans, e.g., because they were trained better.

A surprising finding of this analysis is that target odors can be detected more reliably when the background at a given total concentration c_b consists of many ligands. This can be seen by comparing single-ligand backgrounds (Fig 3A) with multi-ligand backgrounds (Fig 4A), where the effective target concentration is $c_t/c_b = 1/s$. Considering $N_C = 8$, we find $\eta \approx 50\%$ for $c_t/c_b \approx 0.2$ in the single-ligand case, while the ratio can be much smaller ($1/s \approx 0.01$) for multiple ligands. This puzzling result can again be understood in the simplified statistical model, which predicts that the variance of the excitations associated with the background odor is smaller if this odor is comprised of many ligands; see Eq (9) in Methods and Models. This smaller variance implies smaller Δe, so that adding the target has a higher chance of shuffling the order of the excitations to change the primacy set. The same logic implies that the target is easier to detect when the concentrations of the background ligands vary less, which is confirmed by S1 Fig. Taken together, numerical results and the statistical model suggest that a

target odor is easier to notice if the background odor contains many ligands and small concentration variations.

Discriminating similar mixtures. To consider the discrimination of similar odors that have common ligands, we next consider odors that each contain s ligands, sharing s_B of them. Such odors are uncorrelated ($d = d_*$) when they do not share any ligands ($s_B = 0$) and they are identical ($d = 0$) when they share all ligands ($s_B = s$). Between these two extremes, the expected distance d of the primacy sets, and thus the discriminability η, of the two odors can be determined by a numerical ensemble average over sensitivities and by the statistical model; see Methods and Models. Fig 4C shows that both methods predict that more similar odors are harder to discriminate. However, the discriminability of odors only depends on their relative similarity (the fraction of shared ligands) and is independent of the total number of ligands in the odor, consistent with psychophysical experiments [47]. Note however, that our model predicts that basically all mixtures should be easily discriminable, in contrast to the experimental result [47]. This discrepancy might be related to the fact that our model only predicts upper bounds on the encoded information and neglects the decoding in higher regions of the brain.

Identifying odors in a mixtures. So far, we only discussed how well odors can be discriminated, but in reality it is often necessary to identify individual odors in mixtures. To identify ligands, a decoder must compare odor representations to stored patterns. For simplicity, we here only consider a perfect decoder, which associates each representation $\boldsymbol{a}$ with an odor without any uncertainty. This allows us to derive upper bounds for the performance of odor identification without specifying a model for the olfactory processing in the brain. In essence, we use that different odors can only be identified when the associated representations differ, implying that the size of the coding space, $\binom{N_R}{N_C}$, must be large enough to accommodate all odors that need to be distinguished.

We start by considering mixtures of s ligands of equal concentration and ask under what conditions all possible mixtures prepared from a library of N_L ligands are distinguishable, which is the case when $\binom{N_L}{s} < \binom{N_R}{N_C}$. Fig 5A shows that the maximal number N_L^{max} of ligands that could possibly be identified falls off quickly with increasing mixture size s. This analysis implies that if humans were able to identify $N_L = 1000$ ligands, they could do this for mixtures of at most $s = 6$ ligands when the primacy dimension is $N_C = 8$. Note that this is merely an upper bound for the actual performance, since the calculation assumes that the olfactory system is optimized to identify ligands at one particular concentration, whereas natural odors contain ligands at various relative concentrations.

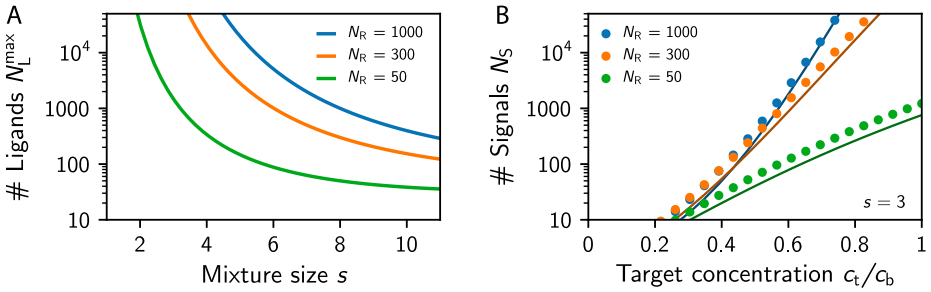

Fig 5. Identifying individual odors in a mixture. (A) Maximal number of ligands, N_L^{max} such that all mixtures of s ligands can be discriminated using various receptor repertoire sizes N_R for $N_C = 8$. (B) Number N_S of ligands that could be distinguished when a ligand of concentration c_t is added to a background of $s = 3$ other ligands at concentration c_b determined from numerical (dots) and analytical (lines) ensemble averages for various N_R and $N_C = 8$. (A,B) Remaining parameters are given in Fig 2A.

https://doi.org/10.1371/journal.pcbi.1007188.g005

To see how concentration variations affect the odor identification, we next use the previously calculated mean distances d between odor representations to estimate how well individual ligands could be detected. In particular, the number of possible ligands that can be distinguished when they are added at concentration c_t to a mixture of s ligands at concentration c_b can be estimated as $\binom{N_R-N_C}{d/2}$, where $\frac{1}{2}d$ is the expected number of the $N_R - N_C$ receptor types that were inactive for the background mixture and became active when the target was added. Fig 5B shows that the number of ligands that can be distinguished in this situation increases strongly with the target concentration $\frac{c_t}{c_b}$. The shown case of $s = 3$ indicates that humans would not be able to identify most ligands if their concentration was half that of the 3 background ligands. Since such concentration fluctuations are very likely to appear in natural situations and in experiments, this suggests that humans realistically can only identify ligands in mixtures of very few components, in line with experimental measurements [48, 49].

The discussion of the identification of odors is limited by the simple description of the decoder in our model. We thus derive upper bounds for the performance, assuming that a mapping of all possible odor combinations to different representations $\boldsymbol{a}$ is possible. This best-case scenario likely requires highly optimized sensitivity matrices S_{ni} and the actual performance might thus lie well below the bounds derived here. However, in realistic olfactory system, the time-course of receptor activation might provide additional information about which ligands are present. For instance, odors from multiple sources might not fully mix and thus arrive in distinguishable whiffs [50].

Primacy coding outperforms alternative coding schemes

We showed that primacy coding contains sufficient information to perform typical olfactory tasks with experimentally measured accuracy. Although this provides some support for primacy coding, alternative encoding schemes might also be consistent with experimental data. To elucidate this, we next compare primacy coding to two alternatives, which are also based on the simple model described by Eqs (1) and (2). The first alternative is binary coding, where glomeruli become active when their excitation exceeds a constant threshold γ [30, 51]. The second alternative is normalized coding, where the threshold is proportional to the mean excitation, $\gamma = \alpha N_R^{-1} \sum_n e_n$, and the inhibition strength α determines how many glomeruli are active on average [21].

To see how binary and normalized coding compare to primacy coding, we calculate the probability η that adding a ligand to a mixture of s ligands can be detected; see Fig 6A. The binary code strongly depends on the overall concentration of the presented odor (or, equivalently, the imposed threshold γ). This implies that there is only a narrow region of mixture sizes s where the binary code allows detecting the addition of a ligand. Conversely, the normalized code is concentration-invariant and could thus in principle discriminate odors at all intensities. However, we showed in Ref. [21] that the encoded information and the discriminability still depend strongly on the mixtures size s in this model. Consequently, normalized codes can only discriminate mixtures of realistic sizes when the inhibition strength α is very low and thus many glomeruli get activated on average.

The example of the normalized code shows that it is not sufficient to study how well different coding schemes can solve olfactory tasks, but one also needs to consider how useful this code is to the downstream decoder. Without modeling the decoder in detail, we here just propose that sparser codes are preferable since they imply fewer firing neurons, which saves energy and simplifies the downstream processing. In fact, sparse coding is typical for sensory information [19, 52]. In our model, the sparsity is given by the fraction $\langle a_n \rangle$ of activated

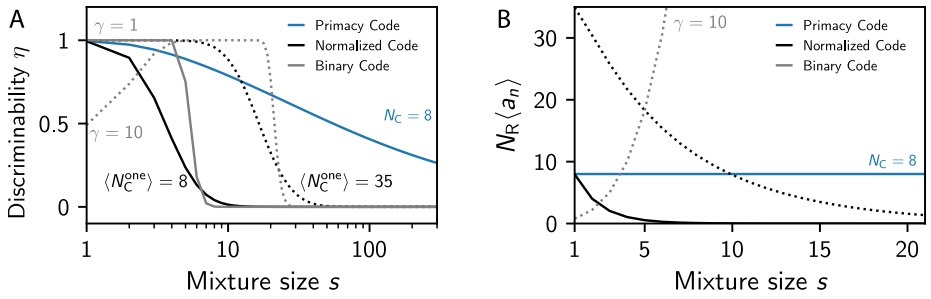

Fig 6. Primacy coding outperforms alternative models. Comparison of the primacy code (blue; $N_C = 8$) to a normalized code (black) and a binary code (gray). In the normalized code, glomeruli are active when their excitation exceeds α times the mean excitation [21]. Here, α is adjusted such that the mean number of glomeruli activated by a single ligand assumes the indicated value $\langle N_C^{one} \rangle$. In the binary code, glomeruli are active when their excitation exceeds the fixed threshold γ [30]. (A) Probability η that adding a ligand to a mixture of s ligands can be detected as a function of s. (B) Representation sparsity, i.e., the mean number of activated glomeruli $N_R \langle a_n \rangle$, as a function of the mixture size s. (A, B) We considered fixed ligand concentrations ($\sigma = 0$) and the remaining parameters are given in Fig 2A.

https://doi.org/10.1371/journal.pcbi.1007188.g006

glomeruli and Fig 6B shows this quantity as a function of the mixture size s. Since larger mixtures imply a higher odor intensity, this number increases quickly in binary coding and makes this code inefficient. Conversely, the number of active glomeruli decreases strongly in normalized coding [21], which explains the poor discriminatory performance for large mixtures. In contrast, primacy coding has a constant sparsity, because it is directly controlled by the primacy count N_C. Taken together, primacy coding outperforms both binary coding and normalized coding essentially because the sparsity of the representation is independent of the presented odors and can thus be adjusted to be useful and efficient over the whole range of possible odors.

The three models discussed here differ in how the statistics of the odor $\boldsymbol{c}$ affect the statistics of the output $\boldsymbol{a}$. In the binary model, the odor intensity given by the mean concentration c_{tot} affects the mean excitation $\langle e_n \rangle$ and therefore the sparsity $\langle a_n \rangle$. This clearly prevents the response from being useful over a wide concentration range. This dependence on the odor intensity is removed in normalized coding, but the variance of the excitations e_n still depends on the odor statistics, e.g. larger mixtures imply smaller variations in e_n. This is problematic since it implies the excitations of fewer glomeruli exceed the fixed threshold in normalized coding, so the sparsity $\langle a_n \rangle$ and the usefulness decrease [21]. In primacy coding, however, the mean activity $\langle a_n \rangle = \frac{N_C}{N_R}$ is independent of the odor statistics, so the system is useful in all situations. In fact, primacy coding can be interpreted as normalized coding with an inhibition strength α that depends on the non-dimensional width of the concentration distribution; see Methods and Models. Primacy coding is thus an example for global inhibition with instantaneous adaptation, which displays better performance than a simple fixed threshold γ. Taken together, this simple model comparison indicates that the mean response of the olfactory systems needs to be controlled and that simple normalization is not sufficient for this.

Overly sensitive receptors degrade the coding efficiency

So far, we calculated the transmitted information and tested the discrimination performance of primacy coding under the assumption that all receptor types behave similarly. In fact, we established that the maximal information is achieved when all receptor types are activated with equal probability N_C/N_R. However, neither the receptor sensitivities nor the odors themselves are distributed equally in realistic situations. Variations in these quantities affect the

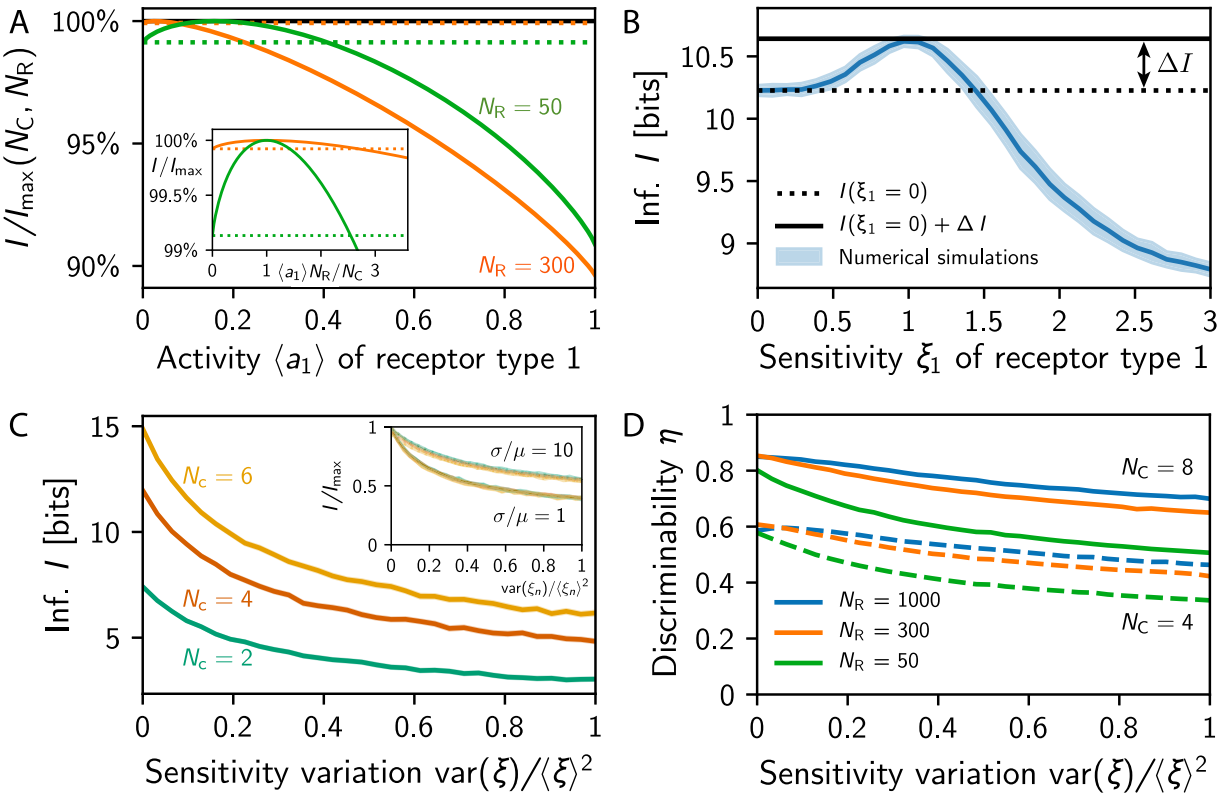

Fig 7. Variations in receptor activities deteriorate the array performance. (A) Information I relative to I_{max} given by Eq (5) as a function of the mean activity $\langle a_1 \rangle$ of the first receptor type while all others are unchanged for $N_C = 8$. Dotted lines indicate $I_{max}(N_C, N_R - 1)$. Inset: Same data for the activity rescaled by N_C/N_R. (B) Numerical simulation of I as a function of the sensitivity factor ξ_1 of the first receptor type for $N_R = 16$, $N_C = 4$, and $\xi_n = 1$ for $n \geq 2$. (C) I for log-normally distributed sensitivity factors ξ_n as a function of $\text{var}(\xi)/\langle \xi \rangle^2$ for various N_C at $N_R = 20$. The inset shows that the scaled information I/I_{max} collapses as a function of $N_R = 10$, 20 and $N_C = 2$, 4, 6 for different widths σ/μ of the concentration distribution. (D) Probability η that adding a ligand to a mixture of $s = 10$ ligands changes the primacy set as a function of $\text{var}(\xi)/\langle \xi \rangle^2$ for various N_R and N_C. (B–D) Shown are numerical simulations with $N_L = 512$, $\mu = \sigma = 1$, and $\lambda = 1$ as well as $s = 16$ in (B,C) and $s = 10$ in (D).

https://doi.org/10.1371/journal.pcbi.1007188.g007

transmitted information and thus the usefulness of the primacy code. For instance, the transmitted information decreases if a single receptor is activated less often than all the others; see Fig 7A. This effect is small, since in the worst case the receptor is never active and the transmitted information thus corresponds to an array with this receptor removed. Conversely, having a receptor that is active more often than all others can have a much more severe effect; see Fig 7A. In fact, if the receptor type is more than three times as active, the transmitted information I is lower than if the receptor type was remove completely; see Methods and Models. This indicates that receptors can shadow the response of other receptors and thus be detrimental to the overall array when they are overly sensitive.

The effect of varying receptor sensitivities can be studied in our model of primacy coding by discussing more general sensitivities matrices. We consider $S_{ni} = \xi_n S^{\text{iid}}_{ni}$, where each receptor type can have a different sensitivity factor ξ_n, which modulates the uniform sensitivity matrix S^{iid}_{ni} where each entry is independently chosen from the same log-normal distribution. The case of homogeneous sensitivities that we discusses so far thus corresponds to $\xi_n = 1$ for $n = 1, 2, \ldots, N_R$.

To investigate the effect of heterogeneous sensitivities, we start by varying the sensitivity factor of one receptor type while keeping all others untouched, i.e., we change ξ_1 while keeping $\xi_n = 1$ for $n \geq 2$. There are three simple limits that we can discuss immediately. For $\xi_1 = 0$, the

first receptor type will never become active, the array behaves as if this type was not present, and the transmitted information is approximately $I_{max}(N_C, N_R - 1)$. This value is lower than the maximally transmitted information $I_{max}(N_C, N_R)$ reached for the symmetric case $\xi_1 = 1$. However, the associated information loss $\Delta I = I_{max}(N_C, N_R) - I_{max}(N_C, N_R - 1) \approx N_C/(N_R \ln 2)$ is relatively small in large receptor arrays ($N_R \gg N_C$); see Fig 7B. Conversely, the transmitted information can be affected much more severely if the sensitivity of the first receptor type is increased beyond $\xi_1 = 1$ and the receptors will thus be active more often than the others. In the extreme case of $\xi_1 \to \infty$, the first receptor type will always be active and thus not contribute any information. Since this receptor type would always be part of the primacy set, the information transmitted by the remaining receptor types is approximately $I_{max}(N_C - 1, N_R - 1)$, which is smaller than $I_{max}(N_C, N_R - 1)$ in the typical case $N_R \gg N_C$. Consequently, an overly active receptor type can be worse than not having this type at all under primacy coding.

The fact that overly sensitive receptors are detrimental to the transmitted information is also visible in numerical simulations. Fig 7B shows ensemble averages of the information I transmitted by receptor arrays as a function of the sensitivity factor ξ_1. As qualitatively argued above, I is maximal for $\xi_1 = 1$ and it is slightly lower for smaller ξ_1 since the receptor type is active less often. In contrast, for $\xi_1 > 1$, I decreases dramatically and falls below the value of $\xi_1 = 0$ for $\xi_1 \gtrsim 1.5$. These data suggest that it would be better to remove receptor types that exhibit a 50% higher sensitivity than the other types.

To see whether overly sensitive receptor types are also detrimental when all types have varying sensitivities, we next considering sensitivity factors ξ_n distributed according to a lognormal distribution. Numerical results shown in Fig 7C indicate that the transmitted information indeed decreases with increasing variance $\mathrm{var}(\xi_n)$ of the sensitivity factors. In fact, a variation of $\mathrm{var}(\xi_n)/\langle\xi_n\rangle^2 = 0.5$ already implies a reduction of the transmitted information by almost 50% for small concentration variations $\sigma/\mu = 1$. If the odor concentrations vary more, the information degradation is less severe, but the same trend is visible. Interestingly, rescaling the information by the maximal information I_{max} given in Eq (5) collapses the curves for all dimensions N_C and N_R, suggesting that this analysis also holds for realistic receptor repertoire sizes. Note that the reduced transmitted information also implies poorer odor discrimination performance; see Fig 7D. Taken together, this provides a strong selective pressure to limit the variability of the receptor sensitivities so overly sensitive receptors do not dominate the whole array.

Discussion

We analyzed a simple model of neural representations of olfactory stimuli, where odors are identified by the N_C strongest responding receptor types. This version of primacy coding provides a sparse representation of the odor identity, which is independent of the odor intensity. We showed using numerical simulations and a statistical model that the primacy dimension N_C strongly affects the transmitted information and the discriminability of odors. Interestingly, already for small values of $N_C \lesssim 10$, the typical olfactory discrimination tasks can be carried out with performances close to experimentally measured ones. Conversely, the number N_R of receptor types does not strongly affect the coding capacity and the discriminability of similar odors, in accordance with lesion experiments. Our model even indicates that lowering N_R can improve the identification of a target ligand in a background.

The advantage of our simple model is that we can analyze its behavior in depth and explicitly link the statistical properties of the olfactory system to data from psycho-physical experiments. In particular, we predict how likely two different odors drawn from a particular statistics can be distinguished. For instance, our model implies that target odors are easier to

detect if disturbing backgrounds consist of many ligands. We generally find that representations are sensitive to the relative concentration of ligands in mixtures and that dilute components are basically completely shadowed. Conversely, for fixed ligand concentrations mixtures can typically be discriminated very well. However, identifying the individual ligands in mixture is only possible for mixtures with few components. In any case, our results suggest that the primacy code formed in the olfactory bulb is more useful to identify odors in the subsequent olfactory cortex than simple alternatives, essentially because the statistics of the representations are independent of the odor statistics.

Our model predicts that receptors are only useful if their likelihood to respond to incoming odors is similar. This is because receptor types that are overly sensitive and respond strongly to many odors could dominate other types and thus degrade the total information. In fact, having a receptor type that is 50% more sensitive than others, and thus responds about three times as often, can lead to less transmitted information than when this type is absent. This observation is related to the primacy hull discussed in [38], which also predicts strong restrictions on the receptor sensitivities stemming from primacy coding. Various strategies could play a role in keeping the activity of the receptor types similar [53]: On timescales as short as a single sniff, the inhibition strength could be adjusted to regulate the relative importance of receptor excitations [54]. On longer timescales of several weeks, there are changes of the receptor copy number that directly affect the sensitivity of the glomeruli [55–57] and the processing neurons in the olfactory bulb [58, 59]. Receptor copy number adaptations influence the signal-to-noise ratio at the receptor level, so the copy number could be increased to improve the detection of frequently appearing odors [60]. In contrast, we predict a decrease of the copy number of overly sensitive receptor types that respond often. Combining the two alternatives, receptor copy numbers could be controlled such that noise is suppressed sufficiently while ensuring that single receptor types do not dominate the array. Finally, receptor sensitivities can also be adjusted by genetic modifications on evolutionary timescales [61, 62]. Moreover, direct feedback from higher regions of the brain could modify the processing of olfactory signals, e.g., in response to the behavioral state [7]. Although our work shows that the activities of the receptors need to be balanced, the actual distribution of the sensitivities matters much less. For instance, log-uniform distributions, which have been suggested to describe realistic receptor arrays [51, 63], lead to similar odor discriminability as log-normally distributed sensitivities; see S2 Fig.

Our results raise the question why mice have 20 times as many receptor types than flies although the transmitted information under primacy coding is only increased by a factor of 2 (see Eq (5)) and the odor discriminability is hardly affected by the receptor repertoire size (see Fig 4). The apparent usefulness of large receptor repertoires hints at roles of the olfactory system beyond transmitting the maximal information and discriminating average odors. For instance, having many receptor types might help to hardwire innate olfactory behavior when receptors are narrowly tuned to odors. In this case, our model would only apply to the fraction of the receptor types that are broadly tuned and are not connected to innate behavior. Alternatively, having many receptor types might be advantageous to discriminate very similar odor mixtures, to cover a larger dynamic range in concentrations of individual ligands, or to allow for a larger variation in average sensitivities, enabling quick adaptation to new environments. Finally, biophysical constraints of the receptor structure might imply that many receptors are required to cover a large part of chemical space.

We discussed the simplest version of primacy coding with a minimal receptor model and a constant primacy dimension N_C implemented by a hard threshold. This model neglects the complex interactions of ligands at the olfactory receptors, which can affect perception [64]. In particular, antagonistic effects can already provide some normalization at the level of receptors

[65]. Generally, it is likely that many mechanisms contribute to the overall normalization of the receptor response [66]. A more realistic model of primacy coding might also consider a softer threshold, where receptor types with larger excitation are given higher weight in the downstream interpretation, which is related to rank coding [22]. In this case, information from fewer glomeruli might be sufficient to identify odors, since the rank carries additional information. Realistic olfactory systems could also use a timing code, taking into account more and more receptor types (with decreasing excitation) until an odor is identified confidently. Such a system could explain that the response dynamics in experiments depend on the task [67, 68]. Generally, a better understanding of the temporal structure of the olfactory code [8, 69–73] might allow to derive more detailed models. These could rely on attractor dynamics that are guided by the excitations and thus respond stronger to the early and large excitations [74, 75].

Methods and models

Numerical simulations

All numerical simulations are based on ensemble averages over sensitivity matrices S_{ni}. The elements of S_{ni} are drawn independently from a log-normal distribution with $\mathrm{var}\,(S_{ni})/\bar{S}^2 = 1.72$ corresponding to $\lambda = 1$. In Figs 2A and 7B–7D, an additional ensemble average over odors $\boldsymbol{c}$ is performed using the distribution $P_{\mathrm{env}}(\boldsymbol{c})$. Here, odors $\boldsymbol{c}$ are chosen by first determining which of the N_{L} ligands are present using a Bernoulli distribution with probability $p = s/N_{\mathrm{L}}$ and then independently drawing their concentration from a log-normal distribution with mean μ and standard deviation σ. In all simulations the primacy set $\boldsymbol{a}$ corresponding to $\boldsymbol{c}$ is given by the N_{C} receptors with the highest excitation calculated from Eq (1). Statistics of $\boldsymbol{a}$ and the transmitted information I given by Eq (4) are determined by repeating this procedure 10^5 and 10^7 times, respectively.

Statistical model

In order to obtain deeper insights into the numerical results, we also develop analytical approximations using a statistical description of all involved quantities, which is based on accounting for the means and variances of the respective distributions. For instance, the statistics of the output $\boldsymbol{a}$ given by Eqs (1)–(3) can be estimated using ensemble averages of sensitivity matrices for different odors $\boldsymbol{c}$, similar to our treatment presented in [21] and [30]. In particular, Eq (1) implies that the effects of different ligands are additive. Since the log-normal distribution describing the sensitivities is narrow ($\lambda = 1$), the excitations e_n are also well approximated by a log-normal distribution with mean $\langle e_n\rangle_S = \bar{S}\sum_i c_i$ and variance and $\mathrm{var}_S(e_n) = \mathrm{var}\,(S_{ni})\sum_i c_i^2$ [76], whereas correlations are negligible [21]. The probability that the excitation e_n exceeds the threshold γ, and the associated receptor type is thus part of the primacy set, reads

$$\langle a_n\rangle_S = 1 - G\left(\frac{\gamma(\boldsymbol{c})}{\langle e_n\rangle_S}; \zeta(\boldsymbol{c})\right) \tag{7}$$

with

$$G(x;\zeta) = \frac{1}{2} + \frac{1}{2}\,\mathrm{erf}\left(\frac{\zeta + \log(x)}{2\zeta^{\frac{1}{2}}}\right) \tag{8}$$

being the cumulative density function of a log-normal distribution with $\langle x\rangle = 1$ and $\mathrm{var}(x) = \exp(2\zeta) - 1$. The width of the distribution is determined by the positive parameter

$\zeta = \frac{1}{2} \ln (1 + \text{var}\,(e_n)/\langle e_n \rangle^2)$, which reads

$$\zeta(\boldsymbol{c}) = \frac{1}{2} \ln \left[1 + \left(e^{\lambda^2} - 1 \right) \frac{\sum_i c_i^2}{\left(\sum_i c_i \right)^2} \right] \tag{9}$$

for an ensemble average over sensitivities. Note that ζ is concentration-invariant, since it does not change when the concentration vector $\boldsymbol{c}$ is multiplied by a constant factor. In the simple case of ligands that are distributed according to $P_{\text{env}}(\boldsymbol{c})$, we find $\langle (\sum_i c_i^2)(\sum_i c_i)^{-2} \rangle_c = s^{-1}(1 + \sigma^2/\mu^2)$. Consequently, the distribution width ζ is large for broadly distributed sensitivities (large λ), few ligands in an odor (small s), and wide concentration distributions (large σ/μ).

The constraint Eq (3) implies $\langle a_n \rangle = N_C/N_R$, so that the mean threshold reads

$$\langle \gamma \rangle = \langle e_n \rangle_S \cdot G^{-1} \left(1 - \frac{N_C}{N_R}; \zeta \right) , \tag{10}$$

where G^{-1} is the inverse function of G defined in Eq (8). Using this expression as an estimate for γ in Eq (7) results in concentration-invariant activities a_n, since $\langle \gamma \rangle$ is proportional to the excitation $\langle e_n \rangle$. This situation is comparable to simple normalized representations resulting from the threshold $\gamma = \alpha \langle e_n \rangle$, where α is a constant inhibition strength [21]. In fact, primacy coding can be interpreted as global inhibition with an inhibition threshold depending on the width of the excitation distribution, $\alpha = G^{-1}(1 - N_C N_R^{-1}; \zeta)$.

Inter-excitation intervals. The expected difference between excitations corresponding to a given odor $\boldsymbol{c}$ can be studied using order statistics, where excitations are re-indexed such that they are ordered, $e_{(1)} < e_{(2)} < \ldots < e_{(N_R)}$. For simplicity, we consider the case where the excitations e_n are distributed identically when considering all odors according to $P_{\text{env}}(\boldsymbol{c})$. Denoting the cumulative distribution function of the excitations by $F(e) = G\left(\frac{e}{\langle e_n \rangle}; \zeta \right)$ and the associated probability density function by $f(e)$, the probability density function associated with the excitation $e_{(n)}$ at rank n reads [77]

$$f_{E_{(n)}}(e) = \frac{N_R!\, f(e)}{(n-1)!\,(N_R - n)!}\, F^{n-1}(e)\, [1 - F(e)]^{N_R - n} . \tag{11}$$

The joint distribution of $E_{(n)}$ and $E_{(m)}$, $1 \leq n < m \leq N_R$, reads [77]

$$\begin{aligned} f_{E_{(n)},E_{(m)}}(e_n, e_m) = {} & \frac{N_R!\, f(e_n) f(e_m)}{(n-1)!(m-n-1)!(N_R - m)!} \\ & \cdot F^{n-1}(e_n)[1 - F(e_m)]^{N_R - m}\, [F(e_m) - F(e_n)]^{m-n-1} . \end{aligned} \tag{12}$$

Consequently, the distribution of the difference $\Delta e = e_{(n)} - e_{(n-1)}$ of consecutive excitations is

$$f_{\Delta E}(\Delta e; n) = \int_0^\infty f_{E_{(n-1)},E_{(n)}}(y, \Delta e + y)\, \mathrm{d}y . \tag{13}$$

Hence, the expected difference $\langle \Delta e \rangle = \int x f_{\Delta E}(x; N_R - N_C - 1)\, \mathrm{d}x$ between the strongest excited inactive receptor type and the weakest active receptor type can be evaluated.

Discriminability of primacy set. The expected number d of changes in the primacy set $\boldsymbol{a}$ when a target odor $\boldsymbol{c}^t$ is added to some background $\boldsymbol{c}^b$ reads

$$d = N_R \cdot (p_{\text{on}} + p_{\text{off}}) , \tag{14}$$

where p_{on} is the probability that a receptor type that was inactive for $\boldsymbol{c}^b$ is turned on by the

perturbation $\boldsymbol{c}^{\mathrm{t}}$ and p_{off} is the probability that a receptor type that was active is turned off. Both probabilities depend on the excitation thresholds $\gamma^{(1)}$ and $\gamma^{(2)}$ associated with the odors $\boldsymbol{c}^{\mathrm{b}}$ and $\boldsymbol{c}^{\mathrm{b}} + \boldsymbol{c}^{\mathrm{t}}$, respectively, which can be estimated from Eq (10) using the respective excitation statistics. With this, p_{on} follows from the probability that the excitation was at the value x below $\gamma^{(1)}$ and the additional excitation by the target brings the total excitation above $\gamma^{(2)}$,

$$p_{\mathrm{on}} \approx \int_0^{\gamma^{(1)}} \left[1 - G\left(\frac{\gamma^{(2)} - x}{\langle e_n^{\mathrm{t}}\rangle_S}; \zeta^{\mathrm{t}}\right)\right] g\left(\frac{x}{\langle e_n^{\mathrm{b}}\rangle_S}; \zeta^{\mathrm{b}}\right) \mathrm{d}x \,, \tag{15}$$

where $g(e; \zeta)$ is the probability density function associated with $G(e; \zeta)$ given in Eq (8). Here, $\langle e_n^j\rangle_S$ and ζ^j describe the excitation statistics of the target (j = t) and the background (j = b). Similarly, we obtain

$$p_{\mathrm{off}} \approx \int_{\gamma^{(1)}}^{\gamma^{(2)}} G\left(\frac{\gamma^{(2)} - x}{\langle e_n^{\mathrm{t}}\rangle_S}; \zeta^{\mathrm{t}}\right) g\left(\frac{x}{\langle e_n^{\mathrm{b}}\rangle_S}; \zeta^{\mathrm{b}}\right) \mathrm{d}x \,, \tag{16}$$

so we can use Eq (14) to calculate the expected Hamming distance d. Note that $\gamma^{(1)}$ and $\gamma^{(2)}$ depend on N_{R}, so the distance d does not scale trivially with N_{R}, in contrast to the case of normalized representations [21].

We use Eqs (14)–(16) to calculate d when a target ligand with concentration c_{t} is added to a background ligand at concentration c_{b}. The associated statistics of the excitations obey

$$\langle e_n^{\mathrm{t}}\rangle_S = \frac{c_{\mathrm{t}}}{c_{\mathrm{b}}} \langle e_n^{\mathrm{b}}\rangle_S \quad \mathrm{var}_S(e_n^{\mathrm{t}}) = \left(\frac{c_{\mathrm{t}}}{c_{\mathrm{b}}}\right)^2 \mathrm{var}_S(e_n^{\mathrm{b}}) \tag{17}$$

and $\mathrm{var}_S(e_n^{\mathrm{b}})/\langle e_n^{\mathrm{b}}\rangle_S^2$ follows from chosen values of σ/μ and λ. Similarly, when a ligand with concentration c is added to a mixture of s ligands, all at concentration c, we have

$$\langle e_n^{\mathrm{t}}\rangle_S = s^{-1} \langle e_n^{\mathrm{b}}\rangle_S \quad \mathrm{var}_S(e_n^{\mathrm{t}}) = s^{-1} \mathrm{var}_S(e_n^{\mathrm{b}}) \,. \tag{18}$$

The third case of correlated odors that we discuss in the main text concerns two odor mixtures of equal size s sharing s_{B} of the ligands. In this case, the excitation threshold γ is the same for both odors and we can express the probability p_{xor} that a receptor type is excited by one mixture but not the other as

$$p_{\mathrm{xor}} = \int_0^{\gamma} G\left(\frac{\gamma - x}{\langle e_n^{\mathrm{D}}\rangle_S}; \zeta^{\mathrm{D}}\right) \left[1 - G\left(\frac{\gamma - x}{\langle e_n^{\mathrm{D}}\rangle_S}; \zeta^{\mathrm{D}}\right)\right] g\left(\frac{x}{\langle e_n^{\mathrm{B}}\rangle_S}; \zeta^{\mathrm{B}}\right) \mathrm{d}x \,, \tag{19}$$

where the parameters $\langle e_n^j\rangle_S$ and ζ^j need to be evaluated for the excitations associated with the s_{B} ligands that are the same (j = B) and the $s - s_{\mathrm{B}}$ ligands that are different (j = D) between the two mixtures. Taken together, the expected distance reads $d = 2N_{\mathrm{R}} p_{\mathrm{xor}}$ and we recover $d = d_*$ for unrelated mixtures ($s_{\mathrm{B}} = 0$) and $d = 0$ for identical mixtures ($s_{\mathrm{B}} = s$).

The calculated distances d between activities can be used to estimate the probability η that the two involved odors can be discriminated. Assuming that glomeruli are independent, the distribution of distances between two activities can be modeled as a binomial distribution over the possible values $\{0, 2, 4, \ldots, 2N_{\mathrm{C}}\}$ with a mean equal to d. The probability η that the representations differ in at least one glomerulus, i.e. that the distance is larger than 0, then reads

$$\eta \approx 1 - \left(1 - \frac{d}{2N_{\mathrm{C}}}\right)^{N_{\mathrm{C}}} \,, \tag{20}$$

which reduces to $\eta \approx 1 - e^{-d/2}$ in the limit $N_{\mathrm{C}} \gg 1$.

Information transmitted by diverse receptors. In the case where the primacy sets $\boldsymbol{a}$ can be partitioned into N_M groups with all elements within a group appearing with the same probability, we can write the information I given by Eq (4) as

$$I = -\sum_{m=1}^{N_M} p_m \log_2\left(\frac{p_m}{M_m}\right), \tag{21}$$

where M_m is the number of elements within group m and p_m is the probability that group m appears in the output, such that $\sum_m M_m = \binom{N_R}{N_C}$ and $\Sigma_m p_m = 1$. In the simple case of one receptor type with deviating statistics, we have $N_M = 2$ with

$$p_1 = \langle a_1 \rangle \quad p_2 = 1 - \langle a_1 \rangle \tag{22a}$$

$$M_1 = \binom{N_R - 1}{N_C - 1} \quad M_2 = \binom{N_R - 1}{N_C} \tag{22b}$$

while the remaining activities are $\langle a_n \rangle = (N_C - \langle a_1 \rangle)/(N_R - 1)$ for $n \geq 2$ to obey Eq (3). For $p_1 = 0$, Eq (21) reduces to $I = I_{max}(N_C, N_R - 1)$, whereas the maximum $I = I_{max}(N_C, N_R)$ is reached for $p_1 = N_C/N_R$. The information decreases for larger p_1 and eventually reaches values lower than $I_{max}(N_C, N_R - 1)$ when $p_1 = p_1^{max}$. For $p_1 > p_1^{max}$, it would thus be advantageous to remove this receptor type. Using $\binom{n}{k} \approx n^k/k!$ and expanding Eq (21) around $p_1 = eN_R/(N_R - 1)$, we find

$$p_1^{max} \approx \frac{1}{\log\left(1 - \frac{eN_C}{N_R - 1}\right) - 1} + 1 = \frac{eN_C}{N_R} + \mathcal{O}\left(\left[\frac{N_C}{N_R}\right]^2\right) \tag{23}$$

in the limit $N_R \gg N_C$ of large repertoires, so $p_1^{max} \approx e\, N_C/N_R$.

Supporting information

S1 Fig. Discrimination of odor mixtures with varying ligand concentrations. Probability η that adding a ligand to a mixture of s ligands changes the primacy set for various N_C. (A) η as a function of s for various widths σ^2/μ^2 of the ligand concentration distribution at $N_R = 300$ and $N_C = 8$. (B,C) η as a function of s for various N_C at $\sigma^2/\mu^2 = 10$. Ensemble averages of the model (colored symbols) are compared to experimental data (black symbols and lines) for (B) humans ($N_R = 300$, data from [45]) and (C) mice ($N_R = 1000$, data from [46]). The right axes display the expected fraction of correct responses in the respective go/no-go experiment. (A–C) Remaining parameters are given in Fig 2A.
(EPS)

S2 Fig. Log-uniform distributed sensitivities behave similar to log-normal distributed ones under primacy coding. (A–B) Probability η that adding a ligand at concentration c_t to a background ligand at concentration c_b changes the primacy set $\boldsymbol{a}$ as a function of c_t/c_b for (A) various N_C at $N_R = 300$ and (B) various N_R at $N_C = 8$. (C) Probability η that adding a ligand to a mixture of s ligands changes the primacy set as a function of s for various N_C and $N_R = 300$. (A–C) Shown are numerical simulations (dots; sample size: 10^5) for $N_L = 512$, $\sigma/\mu = 0$, and $\mathrm{var}(S_{ni})/\bar{S}^2 = 7$, so the log-uniform distributed sensitivities span about 7 orders of magnitude. Note that the three panels are similar to Figs 3A, 3B and 4A, respectively, implying that log-uniform and log-normal distributed S_{ni} behave similarly.
(EPS)

Acknowledgments

I thank Michael P. Brenner, Michael Lässig, Venkatesh N. Murthy, and Mikhail Tikhonov for helpful discussions.

Author Contributions

Conceptualization: David Zwicker.

Formal analysis: David Zwicker.

Investigation: David Zwicker.

Methodology: David Zwicker.

Project administration: David Zwicker.

Software: David Zwicker.

Supervision: David Zwicker.

Validation: David Zwicker.

Visualization: David Zwicker.

Writing – original draft: David Zwicker.

Writing – review & editing: David Zwicker.

References

1. Malnic B, Hirono J, Sato T, Buck LB. Combinatorial receptor codes for odors. Cell. 1999; 96(5):713–723. https://doi.org/10.1016/s0092-8674(00)80581-4 PMID: 10089886
2. Barnes DC, Hofacer RD, Zaman AR, Rennaker RL, Wilson DA. Olfactory perceptual stability and discrimination. Nat Neurosci. 2008; 11(12):1378–80. https://doi.org/10.1038/nn.2217 PMID: 18978781
3. Mathis A, Rokni D, Kapoor V, Bethge M, Murthy VN. Reading out olfactory receptors: feedforward circuits detect odors in mixtures without demixing. Neuron. 2016; 91(5):1110–1123. https://doi.org/10.1016/j.neuron.2016.08.007 PMID: 27593177
4. Tabor R, Yaksi E, Weislogel JM, Friedrich RW. Processing of odor mixtures in the zebrafish olfactory bulb. J Neurosci. 2004; 24(29):6611–20. https://doi.org/10.1523/JNEUROSCI.1834-04.2004 PMID: 15269273
5. Bolding KA, Franks KM. Complementary codes for odor identity and intensity in olfactory cortex. Elife. 2017; 6. https://doi.org/10.7554/eLife.22630 PMID: 28379135
6. Roland B, Deneux T, Franks KM, Bathellier B, Fleischmann A. Odor identity coding by distributed ensembles of neurons in the mouse olfactory cortex. Elife. 2017; 6. https://doi.org/10.7554/eLife.26337 PMID: 28489003
7. Wilson RI. Early olfactory processing in Drosophila: mechanisms and principles. Annu Rev Neurosci. 2013; 36:217–41. https://doi.org/10.1146/annurev-neuro-062111-150533 PMID: 23841839
8. Uchida N, Poo C, Haddad R. Coding and transformations in the olfactory system. Annu Rev Neurosci. 2014; 37:363–85. https://doi.org/10.1146/annurev-neuro-071013-013941 PMID: 24905594
9. Silva Teixeira CS, Cerqueira NMFSA, Silva Ferreira AC. Unravelling the Olfactory Sense: From the Gene to Odor Perception. Chem Senses. 2016; 41(2):105–21. https://doi.org/10.1093/chemse/bjv075 PMID: 26688501
10. Yokoi M, Mori K, Nakanishi S. Refinement of odor molecule tuning by dendrodendritic synaptic inhibition in the olfactory bulb. Proc Natl Acad Sci USA. 1995; 92(8):3371–5. https://doi.org/10.1073/pnas.92.8.3371 PMID: 7724568
11. Berck ME, Khandelwal A, Claus L, Hernandez-Nunez L, Si G, Tabone CJ, et al. The wiring diagram of a glomerular olfactory system. Elife. 2016; 5. https://doi.org/10.7554/eLife.14859 PMID: 27177418
12. Li Z. A model of olfactory adaptation and sensitivity enhancement in the olfactory bulb. Biol Cybern. 1990; 62(4):349–61. https://doi.org/10.1007/BF00201449 PMID: 2310788

13. Li Z. Modeling the sensory computations of the olfactory bulb. In: Models of neural networks. Springer; 1994. p. 221–251.
14. Linster C, Hasselmo M. Modulation of inhibition in a model of olfactory bulb reduces overlap in the neural representation of olfactory stimuli. Behavioural brain research. 1997; 84(1):117–127. https://doi.org/10.1016/S0166-4328(97)83331-1 PMID: 9079778
15. Cleland TA, Sethupathy P. Non-topographical contrast enhancement in the olfactory bulb. BMC Neurosci. 2006; 7:7. https://doi.org/10.1186/1471-2202-7-7 PMID: 16433921
16. Olsen SR, Bhandawat V, Wilson RI. Divisive normalization in olfactory population codes. Neuron. 2010; 66(2):287–99. https://doi.org/10.1016/j.neuron.2010.04.009 PMID: 20435004
17. Zhang D, Li Y, Wu S. Concentration-invariant odor representation in the olfactory system by presynaptic inhibition. Comput Math Methods Med. 2013; 2013:507143. https://doi.org/10.1155/2013/507143 PMID: 23533540
18. Roland B, Jordan R, Sosulski DL, Diodato A, Fukunaga I, Wickersham I, et al. Massive normalization of olfactory bulb output in mice with a'monoclonal nose'. Elife. 2016; 5. https://doi.org/10.7554/eLife.16335 PMID: 27177421
19. Laurent G. A systems perspective on early olfactory coding. Science. 1999; 286(5440):723–8. https://doi.org/10.1126/science.286.5440.723 PMID: 10531051
20. Cleland TA. Early transformations in odor representation. Trends Neurosci. 2010; 33(3):130–139. https://doi.org/10.1016/j.tins.2009.12.004 PMID: 20060600
21. Zwicker D. Normalized Neural Representations of Complex Odors. PLoS One. 2016; 11(11):e0166456. https://doi.org/10.1371/journal.pone.0166456 PMID: 27835696
22. Junek S, Kludt E, Wolf F, Schild D. Olfactory coding with patterns of response latencies. Neuron. 2010; 67(5):872–84. https://doi.org/10.1016/j.neuron.2010.08.005 PMID: 20826317
23. Wesson DW, Carey RM, Verhagen JV, Wachowiak M. Rapid encoding and perception of novel odors in the rat. PLoS Biol. 2008; 6(4):e82. https://doi.org/10.1371/journal.pbio.0060082 PMID: 18399719
24. Wilson CD, Serrano GO, Koulakov AA, Rinberg D. A primacy code for odor identity. Nat Commun. 2017; 8(1):1477. https://doi.org/10.1038/s41467-017-01432-4 PMID: 29133907
25. Paoli M, Albi A, Zanon M, Zanini D, Antolini R, Haase A. Neuronal Response Latencies Encode First Odor Identity Information across Subjects. J Neurosci. 2018; 38(43):9240–9251. https://doi.org/10.1523/JNEUROSCI.0453-18.2018 PMID: 30201774
26. Deconstructing Odorant Identity via Primacy in Dual Networks Kepple Daniel R., Giaffar Hamza, Rinberg Dmitry, and Koulakov Alexei A. Neural Computation 2019 31:4, 710–737
27. Dunkel M, Schmidt U, Struck S, Berger L, Gruening B, Hossbach J, et al. SuperScent–a database of flavors and scents. Nucleic Acids Res. 2009; 37(Database issue):D291–4. https://doi.org/10.1093/nar/gkn695 PMID: 18931377
28. Touhara K, Vosshall LB. Sensing odorants and pheromones with chemosensory receptors. Annu Rev Physiol. 2009; 71:307–32. https://doi.org/10.1146/annurev.physiol.010908.163209 PMID: 19575682
29. Wright GA, Thomson MG. Odor Perception and the Variability in Natural Odor Scenes. In: Romeo J, editor. Integrative Plant Biochemistry. vol. 39 of Recent Advances in Phytochemistry. Elsevier; 2005. p. 191–226.
30. Zwicker D, Murugan A, Brenner MP. Receptor arrays optimized for natural odor statistics. Proc Natl Acad Sci USA. 2016; 113(20):5570–75. https://doi.org/10.1073/pnas.1600357113 PMID: 27102871
31. Verbeurgt C, Wilkin F, Tarabichi M, Gregoire F, Dumont JE, Chatelain P. Profiling of olfactory receptor gene expression in whole human olfactory mucosa. PLOS ONE. 2014; 9(5):e96333. https://doi.org/10.1371/journal.pone.0096333 PMID: 24800820
32. Niimura Y. Olfactory receptor multigene family in vertebrates: from the viewpoint of evolutionary genomics. Curr Genomics. 2012; 13(2):103–14. https://doi.org/10.2174/138920212799860706 PMID: 23024602
33. Su CY, Menuz K, Carlson JR. Olfactory perception: receptors, cells, and circuits. Cell. 2009; 139(1):45–59. https://doi.org/10.1016/j.cell.2009.09.015 PMID: 19804753
34. Silbering AF, Galizia CG. Processing of odor mixtures in the Drosophila antennal lobe reveals both global inhibition and glomerulus-specific interactions. J Neurosci. 2007; 27(44):11966–77. https://doi.org/10.1523/JNEUROSCI.3099-07.2007 PMID: 17978037
35. Mainland JD, Li YR, Zhou T, Liu WLL, Matsunami H. Human olfactory receptor responses to odorants. Sci Data. 2015; 2:150002. https://doi.org/10.1038/sdata.2015.2 PMID: 25977809
36. Münch D, Galizia CG. DoOR 2.0—Comprehensive Mapping of Drosophila melanogaster Odorant Responses. Sci Rep. 2016; 6:21841. https://doi.org/10.1038/srep21841 PMID: 26912260

37. Gao XJ, Clandinin TR, Luo L. Extremely sparse olfactory inputs are sufficient to mediate innate aversion in Drosophila. PLoS One. 2015; 10(4):e0125986. https://doi.org/10.1371/journal.pone.0125986 PMID: 25927233

38. Giaffar H, Rinberg D, Koulakov AA. Primacy model and the evolution of the olfactory receptor repertoire. bioRxiv. 2018; p. 255661.

39. Jefferis GS, Marin EC, Stocker RF, Luo L. Target neuron prespecification in the olfactory map of Drosophila. Nature. 2001; 414(6860):204–8. https://doi.org/10.1038/35102574 PMID: 11719930

40. Cleland TA, Linster C. On-Center/Inhibitory-Surround Decorrelation via Intraglomerular Inhibition in the Olfactory Bulb Glomerular Layer. Front Integr Neurosci. 2012; 6:5. https://doi.org/10.3389/fnint.2012.00005 PMID: 22363271

41. Reisert J, Restrepo D. Molecular tuning of odorant receptors and its implication for odor signal processing. Chem Senses. 2009; 34:535–545. https://doi.org/10.1093/chemse/bjp028 PMID: 19525317

42. Barlow HB. Possible principles underlying the transformations of sensory messages. In: Rosenblith WA, editor. Sensory Communication. MIT press; 1961. p. 217–234.

43. Slotnick B, Bisulco S. Detection and discrimination of carvone enantiomers in rats with olfactory bulb lesions. Neuroscience. 2003; 121(2):451–7. https://doi.org/10.1016/s0306-4522(03)00402-0 PMID: 14522003

44. Bisulco S, Slotnick B. Olfactory discrimination of short chain fatty acids in rats with large bilateral lesions of the olfactory bulbs. Chem Senses. 2003; 28(5):361–70. https://doi.org/10.1093/chemse/28.5.361 PMID: 12826532

45. Jinks A, Laing DG. A limit in the processing of components in odour mixtures. Perception. 1999; 28 (3):395–404. https://doi.org/10.1068/p2898 PMID: 10615476

46. Rokni D, Hemmelder V, Kapoor V, Murthy VN. An olfactory cocktail party: figure-ground segregation of odorants in rodents. Nat Neurosci. 2014; 17(9):1225–32. https://doi.org/10.1038/nn.3775 PMID: 25086608

47. Bushdid C, Magnasco M, Vosshall L, Keller A. Humans can discriminate more than 1 trillion olfactory stimuli. Science. 2014; 343(6177):1370–1372. https://doi.org/10.1126/science.1249168 PMID: 24653035

48. Jinks A, Laing DG. The analysis of odor mixtures by humans: evidence for a configurational process. Physiol Behav. 2001; 72(1-2):51–63. https://doi.org/10.1016/s0031-9384(00)00407-8 PMID: 11239981

49. Goyert HF, Frank ME, Gent JF, Hettinger TP. Characteristic component odors emerge from mixtures after selective adaptation. Brain Res Bull. 2007; 72(1):1–9. https://doi.org/10.1016/j.brainresbull.2006.12.010 PMID: 17303501

50. Kree M, Duplat J, Villermaux E. The mixing of distant sources. Physics of Fluids. 2013; 25(9):091103. https://doi.org/10.1063/1.4820015

51. Koulakov A, Gelperin A, Rinberg D. Olfactory coding with all-or-nothing glomeruli. J Neurophysiol. 2007; 98(6):3134–3142. https://doi.org/10.1152/jn.00560.2007 PMID: 17855585

52. Olshausen BA, Field DJ. Sparse coding of sensory inputs. Curr Opin Neurobiol. 2004; 14(4):481–7. https://doi.org/10.1016/j.conb.2004.07.007 PMID: 15321069

53. Zufall F, Leinders-Zufall T. The cellular and molecular basis of odor adaptation. Chem Senses. 2000; 25 (4):473–81. https://doi.org/10.1093/chemse/25.4.473 PMID: 10944513

54. Hong EJ, Wilson RI. Simultaneous encoding of odors by channels with diverse sensitivity to inhibition. Neuron. 2015; 85(3):573–89. https://doi.org/10.1016/j.neuron.2014.12.040 PMID: 25619655

55. Lazarini F, Lledo PM. Is adult neurogenesis essential for olfaction? Trends Neurosci. 2011; 34(1):20–30. https://doi.org/10.1016/j.tins.2010.09.006 PMID: 20980064

56. Yu CR, Wu Y. Regeneration and rewiring of rodent olfactory sensory neurons. Exp Neurol. 2016;

57. Ibarra-Soria X, Nakahara TS, Lilue J, Jiang Y, Trimmer C, Souza MA, et al. Variation in olfactory neuron repertoires is genetically controlled and environmentally modulated. Elife. 2017; 6. https://doi.org/10.7554/eLife.21476 PMID: 28438259

58. Mouret A, Lepousez G, Gras J, Gabellec MM, Lledo PM. Turnover of newborn olfactory bulb neurons optimizes olfaction. J Neurosci. 2009; 29(39):12302–14. https://doi.org/10.1523/JNEUROSCI.3383-09.2009 PMID: 19793989

59. Liu A, Savya S, Urban NN. Early Odorant Exposure Increases the Number of Mitral and Tufted Cells Associated with a Single Glomerulus. J Neurosci. 2016; 36(46):11646–11653. https://doi.org/10.1523/JNEUROSCI.0654-16.2016 PMID: 27852773

60. Tesileanu T, Cocco S, Monasson R, Balasubramanian V. Environmental adaptation of olfactory receptor distributions. arXiv preprint arXiv:180109300. 2018;.

61. Yu Y, Claire A, Ni MJ, Adipietro KA, Golebiowski J, Matsunami H, et al. Responsiveness of G protein-coupled odorant receptors is partially attributed to the activation mechanism. Proc Natl Acad Sci USA. 2015; 112(48):14966–14971. https://doi.org/10.1073/pnas.1517510112 PMID: 26627247

62. Bear DM, Lassance JM, Hoekstra HE, Datta SR. The Evolving Neural and Genetic Architecture of Vertebrate Olfaction. Curr Biol. 2016; 26(20):R1039–R1049. https://doi.org/10.1016/j.cub.2016.09.011 PMID: 27780046

63. Hopfield J. Odor space and olfactory processing: collective algorithms and neural implementation. Proc Natl Acad Sci USA. 1999; 96(22):12506–12511. https://doi.org/10.1073/pnas.96.22.12506 PMID: 10535952

64. Saraiva LR, Kondoh K, Ye X, Yoon KH, Hernandez M, Buck LB. Combinatorial effects of odorants on mouse behavior. Proc Natl Acad Sci USA. 2016. https://doi.org/10.1073/pnas.1605973113 PMID: 27208093

65. Reddy G, Zak JD, Vergassola M, Murthy VN. Antagonism in olfactory receptor neurons and its implications for the perception of odor mixtures. Elife. 2018; 7. https://doi.org/10.7554/eLife.34958

66. Cleland TA, Chen SYT, Hozer KW, Ukatu HN, Wong KJ, Zheng F. Sequential mechanisms underlying concentration invariance in biological olfaction. Front Neuroeng. 2011; 4:21. https://doi.org/10.3389/fneng.2011.00021 PMID: 22287949

67. Schaefer AT, Margrie TW. Psychophysical properties of odor processing can be quantitatively described by relative action potential latency patterns in mitral and tufted cells. Front Syst Neurosci. 2012; 6:30. https://doi.org/10.3389/fnsys.2012.00030 PMID: 22582039

68. Frederick DE, Brown A, Tacopina S, Mehta N, Vujovic M, Brim E, et al. Task-Dependent Behavioral Dynamics Make the Case for Temporal Integration in Multiple Strategies during Odor Processing. J Neurosci. 2017; 37(16):4416–4426. https://doi.org/10.1523/JNEUROSCI.1797-16.2017 PMID: 28336570

69. Egea-Weiss A, Kleineidam CJ, Szyszka P, et al. High Precision of Spike Timing across Olfactory Receptor Neurons Allows Rapid Odor Coding in Drosophila. iScience. 2018; 4:76–83. https://doi.org/10.1016/j.isci.2018.05.009 PMID: 30240755

70. Gupta P, Albeanu DF, Bhalla US. Olfactory bulb coding of odors, mixtures and sniffs is a linear sum of odor time profiles. Nat Neurosci. 2015; 18(2):272–81. https://doi.org/10.1038/nn.3913 PMID: 25581362

71. Blauvelt DG, Sato TF, Wienisch M, Murthy VN. Distinct spatiotemporal activity in principal neurons of the mouse olfactory bulb in anesthetized and awake states. Frontiers in neural circuits. 2013; 7(46). https://doi.org/10.3389/fncir.2013.00046 PMID: 23543674

72. Spors H, Wachowiak M, Cohen LB, Friedrich RW. Temporal dynamics and latency patterns of receptor neuron input to the olfactory bulb. J Neurosci. 2006; 26(4):1247–59. https://doi.org/10.1523/JNEUROSCI.3100-05.2006 PMID: 16436612

73. Hopfield JJ. Pattern recognition computation using action potential timing for stimulus representation. Nature. 1995; 376(6535):33–6. https://doi.org/10.1038/376033a0 PMID: 7596429

74. Herman PA, Benjaminsson S, Lansner A. Odor recognition in an attractor network model of the mammalian olfactory cortex. In: Neural Networks (IJCNN), 2017 International Joint Conference on. IEEE; 2017. p. 3561–3568.

75. Grabska-Barwińska A, Barthelmé S, Beck J, Mainen ZF, Pouget A, Latham PE. A probabilistic approach to demixing odors. Nat Neurosci. 2016; 20:98–106. https://doi.org/10.1038/nn.4444 PMID: 27918530

76. Fenton LF. The sum of log-normal probability distributions in scatter transmission systems. Communications Systems, IRE Transactions on. 1960; 8(1):57–67. https://doi.org/10.1109/TCOM.1960.1097606

77. David HA, Nagaraja HN. Order statistics. Wiley Online Library; 1970.